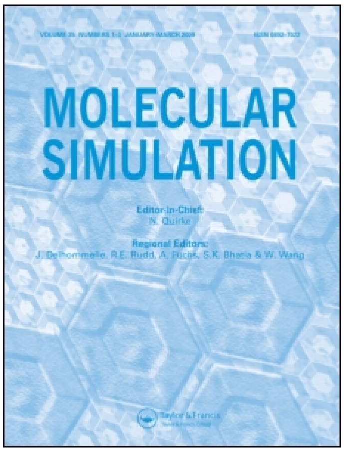

Molecular Simulation

Publication details, including instructions for authors and subscription information:
http://www.informaworld.com/smpp/title~content=t713644482

Tight-binding Molecular Dynamics Simulation of Uniaxial Tensile Strength of Diamond

Tamotsu Hashimoto[a]
[a] Material Structural Formation Process Department, National Industrial Research Institute of Nagoya, Japan

To cite this Article Hashimoto, Tamotsu(1999) 'Tight-binding Molecular Dynamics Simulation of Uniaxial Tensile Strength of Diamond', Molecular Simulation, 23: 2, 143 — 150

To link to this Article: DOI: 10.1080/08927029908022118

URL: http://dx.doi.org/10.1080/08927029908022118

Molecular Simulation, 1999, Vol. 23, pp. 143-150
Reprints available directly from the publisher
Photocopying permitted by license only

Published by license under
the Gordon and Breach Science
Publishers imprint.
Printed in Malaysia.

TIGHT-BINDING MOLECULAR DYNAMICS SIMULATION OF UNIAXIAL TENSILE STRENGTH OF DIAMOND

TAMOTSU HASHIMOTO

Material Structural Formation Process Department, National Industrial Research Institute of Nagoya, 462-8510 Japan

(Received June 1999; accepted June 1999)

Tight-binding molecular dynamics simulations have been performed to study the ideal strength of diamond under a uniaxial [111] tensile load with stresses treated by Parrinello-Rahman method. The stress-stretch relationships and Poisson contractions for single crystalline diamond with and without vacancies, and diamond containing $\{111\}\Sigma = 3$ boundaries at 300 K were calculated. I estimated the ideal strength of diamond to be $\sim$230 GPa at critical stretch $\sim$1.31.

Keywords: Tight-binding molecular dynamics simulation; ideal strength; stress-stretch relationships; Poisson contractions; vacancy; $\{111\}\Sigma = 3$ boundary

1. INTRODUCTION

Diamonds usually cleave along one particular (111) plane [1, 2]. The reason is not clear, but it is deduced that since (111) plane is the growth plane, it will contain layers of faulted growth, and the defects on the (111) plane give preferential weakening [3]. Therefore, it is interesting to know the strength without any defects (the ideal strength) of diamond on [111] tensile load by calculations and compare the result with results calculated under various conditions of containing simple defects such as vacancies and boundaries.

Ideal [111] tensile strength [4] of diamond $\sigma_{\max}$ has been calculated previously. One way of calculation is to use Morse function

$\phi(r) = \phi_0[(\exp\{-a(r-r_0)\}-1)^2-1]$, where r_0, ϕ_0 and a, are parameters which are determined from the equilibrium carbon–carbon distance, the binding energy, and a characteristic adsorption frequency determined spectroscopically, respectively. The force required to break one such bond is the maximum slope of the Morse function. From the value of this force and the number of bonds per unit area, one can calculate $\sigma_{\max}$. By this method, Tyson [5] predicted $\sigma_{\max}$ to be 106 GPa, and Kelly *et al.* [6] predicted $\sigma_{\max}$ to be 140 GPa. Another way of calculation is to use Orowan's formula [7], which relate the ideal strength of a solid directly to other macroscopic physical properties, $\sigma_{\max} = (E\gamma/a_0)^{1/2}$, where E, γ, and a_0 are Young's modulus, surface energy, and interplanar spacing of the planes perpendicular to the tensile axis, respectively. By this method, Kelly [8] predicted $\sigma_{\max}$ to be 205 GPa, and using different values of E, γ, and a_0, Field [3] predicted it to be 190 GPa. By using a recent atomistic bond orbital model, Uemura [9] predicted $\sigma_{\max}$ to be 80 GPa.

Since these calculated values differ largely, it is meaningful to obtain $\sigma_{\max}$ by more reliable calculations. Because of this reason, we calculated the ideal strength $\sigma_{\max}$ by tight-binding molecular dynamics simulation. I used a tight-binding model by Xu *et al.* [10], which correctly represents the energy-volume curves for diamond, graphite, and linear chain of carbon atoms. This model is widely used in the study of various carbon systems such as liquid carbon, amorphous carbon, and fullerenes [11], proving that the model can describe carbon systems over a wide range of bonding environments. I assumed that this model could also represent the stress-stretch relations of diamond by the uniaxial [111] tensile load and applied the model to the study of the ideal strength of diamond.

I used Parrinello–Rahman method for stress control [12]. By this method, the effect of Poisson contraction is included in our calculations. Parrinello–Rahman method is used in classical molecular dynamics simulations on structural phase transformations of solids [13] and in first-principles molecular dynamics simulations on structural phase transformations to high pressure phases of Si [14, 15] or C [16]. I have applied this method to constant stress tight-binding molecular dynamics simulations. I calculated stress-stretch relationships for single crystalline diamond with and without vacancies, and diamond containing $\{111\}\Sigma = 3$ grain boundaries, a typical grain boundaries in CVD diamond films [17]. By our calculations, the ideal strength of diamond was estimated to be $\sim$230 GPa.

2. METHOD

The Lagrangian I used is

$$L = \frac{1}{2}\sum_i m_i \dot{\mathbf{s}}_i^t \mathbf{G} \dot{\mathbf{s}}_i - 2\sum_n^{(\mathrm{occup})} \varepsilon_n - U_{\mathrm{rep}} + \frac{1}{2} W \mathrm{Tr} \dot{\mathbf{h}}^t \dot{\mathbf{h}} - p\Omega - \frac{1}{2}\mathrm{Tr}\boldsymbol{\Sigma}\mathbf{G}, \tag{1}$$

where

$$\boldsymbol{\Sigma} = \mathbf{h}_0^{-1}(\mathbf{S} - p)\mathbf{h}_0^{-1t}\Omega_0. \tag{2}$$

I used tight-binding total energy in the ordinary Parrinello–Rahman Lagrangian [12]. The first term is the kinetic energy of atoms, where the i-th atom's position $\mathbf{r}_i$ is scaled such as $\mathbf{r}_i = \mathbf{h}\mathbf{s}_i$, where $\mathbf{h}(t) = \{\mathbf{a}, \mathbf{b}, \mathbf{c}\}$ (the three vectors **a**, **b**, and **c** span the edges of the MD cell). $\mathbf{G} = \mathbf{h}^t\mathbf{h}$. The second term is the band structure energy and contains a factor 2 to take into account the spin degeneracy. The superscript (occup) indicates that I use just those electron energies ε_n belonging to the lower half spectrum of the TB matrix. The third term is the repulsive potential. The fourth term is the kinetic energy of the MD cell. In the fifth term, p is the externally applied hydrostatic pressure and Ω is the volume of the MD cell. The last term is the elastic energy, where $\boldsymbol{\Sigma}$ is related to the stress tensor S by Eq. (2). $\mathbf{h}_0$ and Ω_0 are $\langle \mathbf{h} \rangle$ and $\langle \Omega \rangle$ in an equilibrium state, respectively. The values of W and p in the Lagrangian were 10 atomic mass unit and 0 GPa, respectively, throughout this simulation. The fifth order Gear predictor-corrector method was used for numerical computation [18]. The time step used to solve the equation of motion was $\Delta t = 0.7$ fs.

3. RESULTS

I have calculated on three models of diamond, that is, single crystalline diamond with and without a vacancy in a unit cell, and diamond containing two $\{111\}\Sigma = 3$ boundaries in a unit cell. For single crystalline diamond with and without vacancies (Fig. 1(a)), I used 143 and 144 carbon atoms, respectively. In the latter case, a unit cell contains 12 carbon layers, each layer containing 12 carbon atoms. The tensile direction was [111] for these two models. For diamond containing $\{111\}\ \boldsymbol{\Sigma} = 3$ boundaries (Fig. 1(b)), I

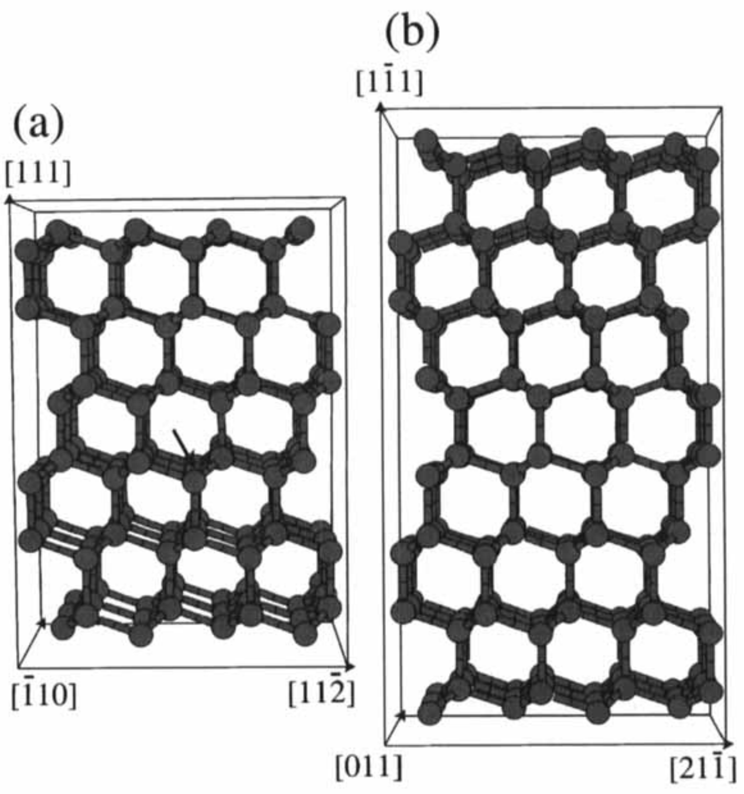

FIGURE 1 Initial atomic configurations for single crystalline diamond with and without a vacancy in a unit cell (a) and diamond containing two $\{111\}\Sigma = 3$ boundaries in a unit cell (b). The arrow in the figure of single crystalline diamond represents the vacancy position. The unit cell edges are also shown in both figures.

used 192 carbon atoms. In this case, a unit cell contains 16 carbon layers, each layer containing 12 carbon atoms. The tensile direction was $[1\bar{1}1]$ for this model.

Figure 2(a) shows stress-stretch relationships for the three models. Each data point was calculated at constant stress and constant temperature of 300 K and averaged for 2000 Δt. I obtained the values of stresses and stretches by changing Σ_{33} from 0 to a value at which the system failed by -1, other matrix elements of $\mathbf{\Sigma}$ being kept 0. Near the critical stretch, I changed Σ_{33} typically by -0.1. The critical values of Σ_{33}'s corresponding to the critical stresses below which the systems failed were $\Sigma_{33} = -5.77$, -4.9, and -4.4 for single crystalline diamond with no vacancies, single crystalline diamond with vacancies, and diamond containing $\{111\}\Sigma = 3$

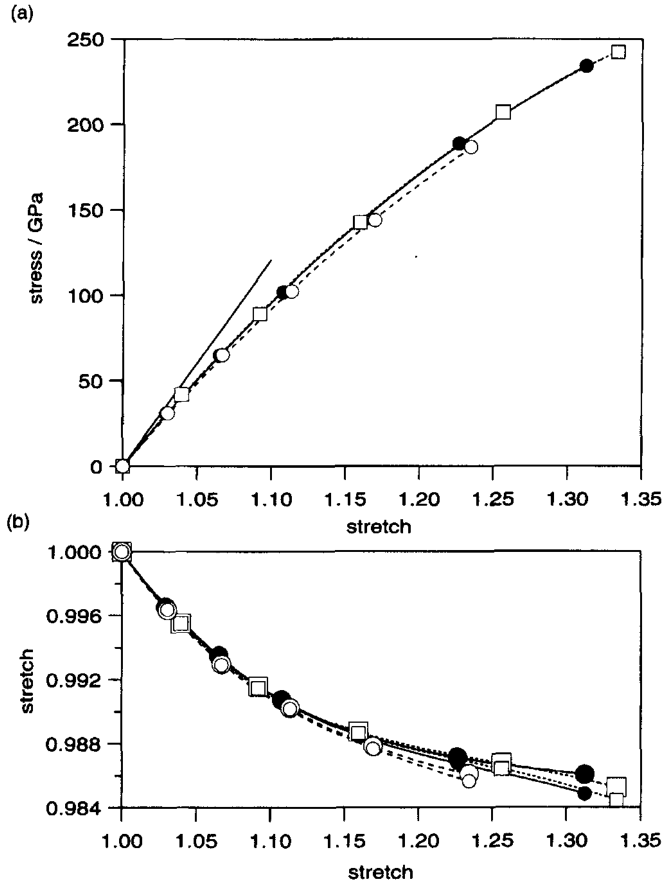

FIGURE 2 Stress-stretch relations (a) and Poisson contractions (b) for single crystalline diamond with no vacancy (black circle), single crystalline diamond with one vacancy in the unit cell (white circle), and diamond containing $\{111\}\Sigma = 3$ boundaries (white square). The slope of the straight line in the figure of stress-stretch relations represents Young's modulus by an experiment (1207 GPa). In the figure of Poisson contractions, the larger circles represent stretches to the $[11\bar{2}]$ directions, the smaller circles represent stretches to the $[\bar{1}10]$ directions, the larger squares represent stretches to the $[21\bar{1}]$ directions, and the smaller squares represent stretches to the $[011]$ directions.

boundaries, respectively. I fitted the obtained data points by the following polynomial: $\sigma = a(x-1)(b(x-1)-1)^2$. For single crystalline diamond with no vacancy, the values of a and b were 1061 and 0.5095, respectively. The curves for single crystalline diamond and that for diamond containing $\{111\}\Sigma = 3$ boundaries are almost the same. The curve is more linear than that for SiC obtained by *ab initio* calculations [19]. In Figure 2(a), it is shown that the model for diamond with vacancies stretches longer than the other two models when the same stresses are applied. This is because of the high vacancy density of the model (one vacancy per 12 carbon atoms in a layer containing vacancies as shown in Fig. 1(a)).

The values of Young's modulus for the corresponding tensile directions were 1074, 1061, and 1020 GPa for diamond containing $\{111\}\Sigma = 3$ boundaries, single crystalline diamond with no vacancies, and single crystalline diamond with vacancies, respectively. The present value 1061 GPa for single crystalline diamond is smaller than an experimental value 1207 GPa [20] (the slope of the straight line in Fig. 2(a)) calculated using a relationship between Young's modulus and stiffnesses c_{11}, c_{12}, and c_{44} [21] by 12%.

The critical strengths were 242, 234, and 187 GPa at critical stretches 1.33, 1.31, and 1.23 for diamond containing $\{111\}\Sigma = 3$ boundaries, single crystalline diamond with no vacancies, and single crystalline diamond with vacancies, respectively. The predicted critical strength for single crystalline diamond with no vacancy was larger than any of other calculations [3, 5–9]. The value was close to the values obtained using Orowan's formula [3, 7, 8]. The tight-binding model I used predicts hexagonal diamond more stable than cubic method by 0.007 eV/atom [17]. Because the $\{111\}\Sigma = 3$ boundary contains the same stacking sequence as hexagonal diamond, the model for diamond containing $\{111\}\Sigma = 3$ boundaries was more stable than the model for cubic single crystalline diamond up to a largely stretched state. The critical strength of diamond with vacancies by our model was 20% smaller than that of single crystalline diamond with no vacancies.

Figure 2(b) shows Poisson contractions for the three cases. I fitted the calculated data points by 4-th order polynomials. By an experiment, Poisson's ratio of diamond by [111] tensile load is evaluated to be 0.045 [8, 20]. By our calculations, the value was 0.13 for single crystalline diamond with no vacancies and diamond containing $\{111\}\Sigma = 3$ boundaries for both directions of the unit cell edges perpendicular to the tensile directions. The value was 0.14 for diamond with vacancies for both directions of the unit cell edges perpendicular to the tensile direction. As seen from Figure 2(b), the maximum contractions for all the three cases were less than 1.6%. The curves for single crystalline diamond with no vacancies and diamond containing $\{111\}\Sigma = 3$ boundaries are similar, as the stress-stretch relationships for them were similar. Diamond with vacancies by this model contracts more than the other two cases. At largely stretched states, contractions tended to be direction dependent for all the three cases. However, the difference between the values of contractions for the two unit cell edges for each case is small. For example, in the case of single crystalline diamond with no vacancy, the difference between the values of contractions for the two unit cell edges at the largest strain in Figure 2(b) is about 0.0013.

4. CONCLUSION

By tight-binding molecular dynamics simulations using Parrinello – Rahman method, I investigated stress-stretch relationships and Poisson contractions for single crystalline diamond with and without vacancies, and diamond containing $\{111\}\Sigma = 3$ boundaries at 300 K. I obtained the following results:

(1) $\sigma_{\max}$ of single crystalline diamond Using a model by Xu *et al.* [10], I estimated ideal strength $\sigma_{\max}$ of diamond by [111] tensile load to be ~ 230 GPa at critical stretch ~ 1.31. The value for $\sigma_{\max}$ is close to the values estimated using Orowan's formula [3, 7, 8].

(2) Effects of $\{111\}\Sigma = 3$ boundaries For both curves of stress-stretch relationships and Poisson contractions, the difference was small between single crystalline diamond with no vacancies and diamond containing $\{111\}\Sigma = 3$ boundaries. The latter was a little (3.4%) more stable up to a largely stretched state than the former presumably because the tight-binding model predicts hexagonal diamond more stable than cubic diamond [17].

(3) Effects of vacancies Because the density of vacancies in our model for single crystalline diamond with vacancies is high (one vacancy per 12 carbon atoms in a layer containing vacancies), it stretches in the tensile direction and contracts in the directions perpendicular to the tensile direction more easily than in the case of single crystalline diamond without vacancies. The ctitical strength of diamond with vacancies decreased largely (by 20%) compared to diamond with no vacancies.

Acknowledgments

This work was supported by STA of Japan. I thank Dr. T. Oda for providing the original version of tight-binding MD source code and useful discussions. I thank Dr. H. Ogawa and Dr. N. Sawaguchi for useful discussions.

References

[1] Ansell, M. F. (1984). "Diamond cleavage", *Chemistry in Britain*, **20**, 1017.
[2] Field, J. E. and Freeman, C. J. (1981). "Strength and fracture properties of diamond", *Philos. Mag. A*, **43**, 595.

[3] Field, J. E., "Strength, fracture and erosion properties of diamond", In: *The properties of natural and synthetic diamond*, Edited by Field, J. E. (Academic, New York, 1992).
[4] Macmillan, N. H. (1972). "Review: The theoretical strength of Solids", *Journal of Materials Science*, **7**, 239.
[5] Tyson, W. R. (1966). "Theoretical strength of perfect crystals", *Philos. Mag.*, **14**, 925.
[6] Kelly, A., Tyson, W. R. and Cottrell, A. H. (1967). "Ductile and brittle crystals", *Philos. Mag.*, **15**, 567.
[7] Orowan, E. (1949). "Fracture and strength of solids", *Rep. Prog. Phys.*, **12**, 185.
[8] Kelly, A. and Macmillan, M. H., In: Strong Solids 3rd edn. (Oxford University Press, New York, 1986).
[9] Uemura, Y. (1994). "Atomistic model for the evaluation of the stability of diamond under uniaxial tensile force", *Phys. Rev.*, **B49**, 6528.
[10] Xu, C. H., Wang, C. Z., Chan, C. T. and Ho, K. M. (1992). "A transferable tight-binding potential for carbon", *J. Phys.: Condens. Matter*, **4**, 6047.
[11] Wang, C. Z. and Ho, K. M. (1997). "Material simulations with tight-binding molecular dynamics", *Journal of Phase Equilibria*, **18**, 516.
[12] Parrinello, M. and Rahman, A. (1981). "Polymorphic transitions in single crystals: A new molecular dynamics method", *J. Appl. Phys.*, **52**, 7182.
[13] Hashimoto, T., Sugawara, S. and Hiwatari, Y. (1997). "Structural transformation of ice at normal and high pressures via molecular dynamics simulations", *J. Phys. Chem.*, **B101**, 6293.
[14] Focher, P., Chiarotti, G. L., Bernasconi, M., Tosatti, E. and Parrinello, M. (1994). "Structural phase transformation via first-principles simulation", *Europhys. Lett.*, **26**, 345.
[15] Bernasconi, M., Chiarotti, G. L., Focher, P., Scandolo, S., Tosatti, E. and Parrinello, M. (1995). "First-principle-constant pressure molecular dynamics", *J. Phys. Chem. Solids*, **56**, 501.
[16] Scandolo, S., Chiarotti, G. L. and Tosatti, E. (1996). "Stability of diamond at megabar pressures", *Phys. Stat. Sol. (b)*, **198**, 447.
[17] Kohyama, M., Ichinose, H., Ishida, Y. and Nakanose, M. (1994). "Energies and atomic structures of grain boundaries in diamond: comparison with grain boundaries in silicon", *Mat. Res. Soc. Symp. Proc.*, **339**, 681.
[18] van Gunsteren, W. F. and Berendsen, H. J. C. (1977). "Algorithms for macromolecular dynamics and constraint dynamics", *Mole. Phys.*, **34**, 1311.
[19] Li, W. and Wang, T. (1999). "Elasticity, stability, and ideal strength of β-SiC in plane-wave-based ab initio calculations", *Phys. Rev.*, **B59**, 3993.
[20] Grimsditch, M. H. and Ramdas, A. K. (1975). "Brillouin scattering in diamond", *Phys. Rev. B*, **11**, 3139.
[21] Nye, J. F., Physical properties of crystals (Oxford University Press, London, 1964), Chap. 8.